



# WOCE NOTES

## The U.S. role in the World Ocean Circulation Experiment

Vol. 5 No. 2  
April 1993

### **Notes on the S. Pacific hydrographic section near 32°S—WHP P6**

*By Michael S. McCartney and Molly O'Neil Baringer, Woods Hole Oceanographic Institution*

In late April 1993 the renovated R/V *Knorr* will leave the South Pacific Ocean through the Panama Canal and enter the Atlantic after almost one year of Pacific work, dedicated predominately to U.S. WOCE. This extended voyage (number 138) included the deployment of U.S. WOCE mooring PCM11 and the occupation of U.S. WOCE Hydrographic Program (WHP) lines P6, P14C, P17A, P17E, P16S, and, as we are writing, P19.

The first Pacific cruise occupied by the refit *Knorr* was line P6, a South Pacific transect near 32°S. P6 work commenced from Valparaiso,

Chile, on 2 May 1992 and ended at Sydney, Australia, almost three months later on 30 July 1992. The transect was broken into three legs by a four day stop at Easter Island at the end of May and a six day stop in Wellington, New Zealand, at the beginning of July. Harry Bryden (WHOI) was chief scientist on the first leg, P6E; Mike McCartney on the second, P6C; and John Toole (WHOI) and John Church (CSIRO) on the third, P6W, a joint U.S./Australian effort.

The P6 cruise track is shown in Figure 1 (p. 4). The section consisted of 267 full water column stations, including seven stations made for

*(continued on page 4)*

(P6, continued from first page)

instrument tests and to overlap legs and twenty repeat stations along the East Australian Current. The widest station spacing was planned at 34 nm in the interior; various circumstances combined to force an expansion to 42 nm for the longitude range 141°W–160°W. P6 sampling included the full suite of water sampling from the thirty-six bottle rosette system and deployment of surface drifters and Autonomous Lagrangian Circulation Explorer (ALACE) floats; no large volume sampling was made. After completing the line, investigators twice repeated the western end, westward from 155°E, to gain additional East Australian Current samples to compliment the moored current meter array, PCM3, located along this part of the section. Also of note is the section's placement over the deep western boundary current array, PCM9, extending eastward from the Kermadec Ridge to near 167°W.

We provide below preliminary interpretations, with a focus on the area east of the international date line. We acknowledge the disparate data analysis products shown here; a more coherent style of visualization should evolve with continued analysis.

### The deep boundary current in the central South Pacific

Warren (1973) estimated the magnitude of deep transport at 28°S and 43°S during the Scorpio expedition. The principal deep western boundary current (DWBC), that of the Southwest Pacific Basin, below 2000 m was estimated to transport about  $19 \times 10^6 \text{ m}^3 \text{ s}^{-1}$  at both sections, with a substantial ( $11 \times 10^6 \text{ m}^3 \text{ s}^{-1}$ ) superimposed gyre flow over the Kermadec Trench at 28°S. Net deep transports were estimated as  $11.6 \times 10^6 \text{ m}^3 \text{ s}^{-1}$  at 43°S east of New Zealand and as  $15.3 \times 10^6 \text{ m}^3 \text{ s}^{-1}$  at 28°S east of the Kermadec Ridge. For the 32°S section we use the same reference level as Warren. Applying a level of no motion at 2000 db yields a DWBC transport of  $25.5 \times 10^6 \text{ m}^3 \text{ s}^{-1}$  and a net transport east of the Kermadec Ridge of  $22.4 \times 10^6 \text{ m}^3 \text{ s}^{-1}$ . It is unknown if these larger transports, as

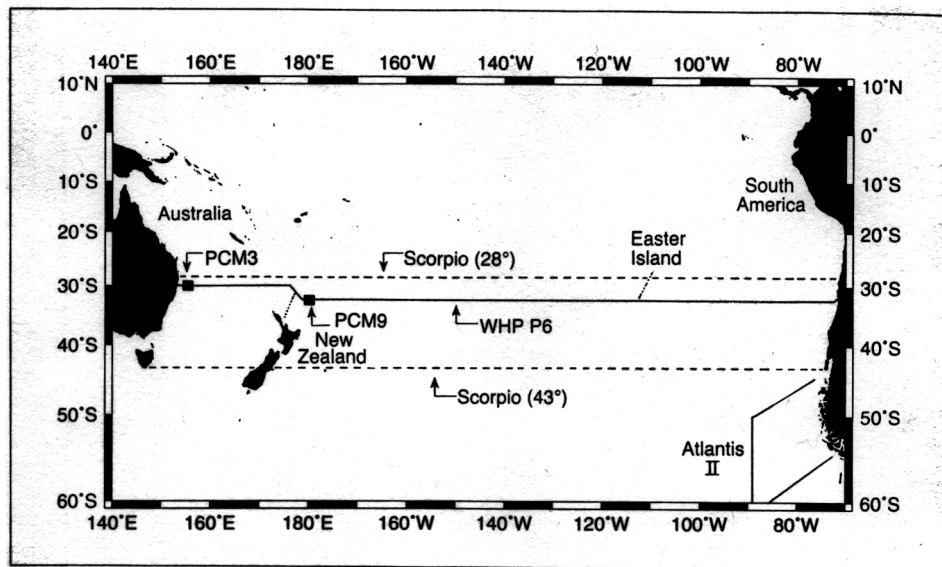


Figure 1. Cruise track for WHP section P6 near 32°S. Also shown are the locations of the Scorpio Expedition sections near 28°S and 43°S (data shown in Figure 3), the locations of the winter 1980 Atlantis II survey (data shown in Figure 4), and the approximate locations of WOCE moorings PCM3 and PCM9.

compared to the Scorpio sections, reflect the details of level of no motion determination, a stronger abyssal circulation at 32°S than at the other two locations, a low frequency transport variability, or a combination of all three factors.

As an indication of the sensitivity of these transport estimates to the level of no motion, shifting to 1700 db would lower the DWBC and net transport estimates to  $19.9 \times 10^6 \text{ m}^3 \text{ s}^{-1}$  and  $13.4 \times 10^6 \text{ m}^3 \text{ s}^{-1}$  (below 2000 db). Shifting still shallower to 1500 db would reduce the estimates to  $15 \times 10^6 \text{ m}^3 \text{ s}^{-1}$  and  $5 \times 10^6 \text{ m}^3 \text{ s}^{-1}$ . This sensitivity reflects the existence of a deep penetration of the subtropical thermocline bowl, and the conversion of its corresponding shear from a northward subtropical gyre flow to a southward deep flow as the reference level is elevated into the bowl. This is, of course, related to Reid's (1973) suggestion of southward flow at mid-depth.

A first cut at a spatially variable level of no motion worked out by John Toole to reflect various plausible constraints on flow directions for specific circulation

elements gives  $21.2 \times 10^6 \text{ m}^3 \text{ s}^{-1}$  and  $17.3 \times 10^6 \text{ m}^3 \text{ s}^{-1}$ . Much additional work remains to resolve the reference level issue for the section as a whole in the context of the total South Pacific circulation. Figure 2a shows the transport below 2000 db accumulated westward along the section for Toole's level of no motion. We point out next a few of the principal circulation elements that this distribution reveals.

A clockwise gyre flow (cyclonic in the southern hemisphere) over the Chile Basin is visible, with an amplitude of about  $5 \times 10^6 \text{ m}^3 \text{ s}^{-1}$ , but with only a weak net flow. There is perhaps about  $1 \times 10^6 \text{ m}^3 \text{ s}^{-1}$  net northward flow east of 112°W, the crest of the east Pacific Rise, with the western gyre limb a broad basin-scale northward flow, and the eastern limb a narrow southward flow at the eastern boundary over the Chile Trench.

There is little circulation indicated over the broad crown of the East Pacific Rise between 90°W and 130°W, where the depths are mostly shallower than 4000 m. Descending the western flank of the Rise westward from 130°W, activity

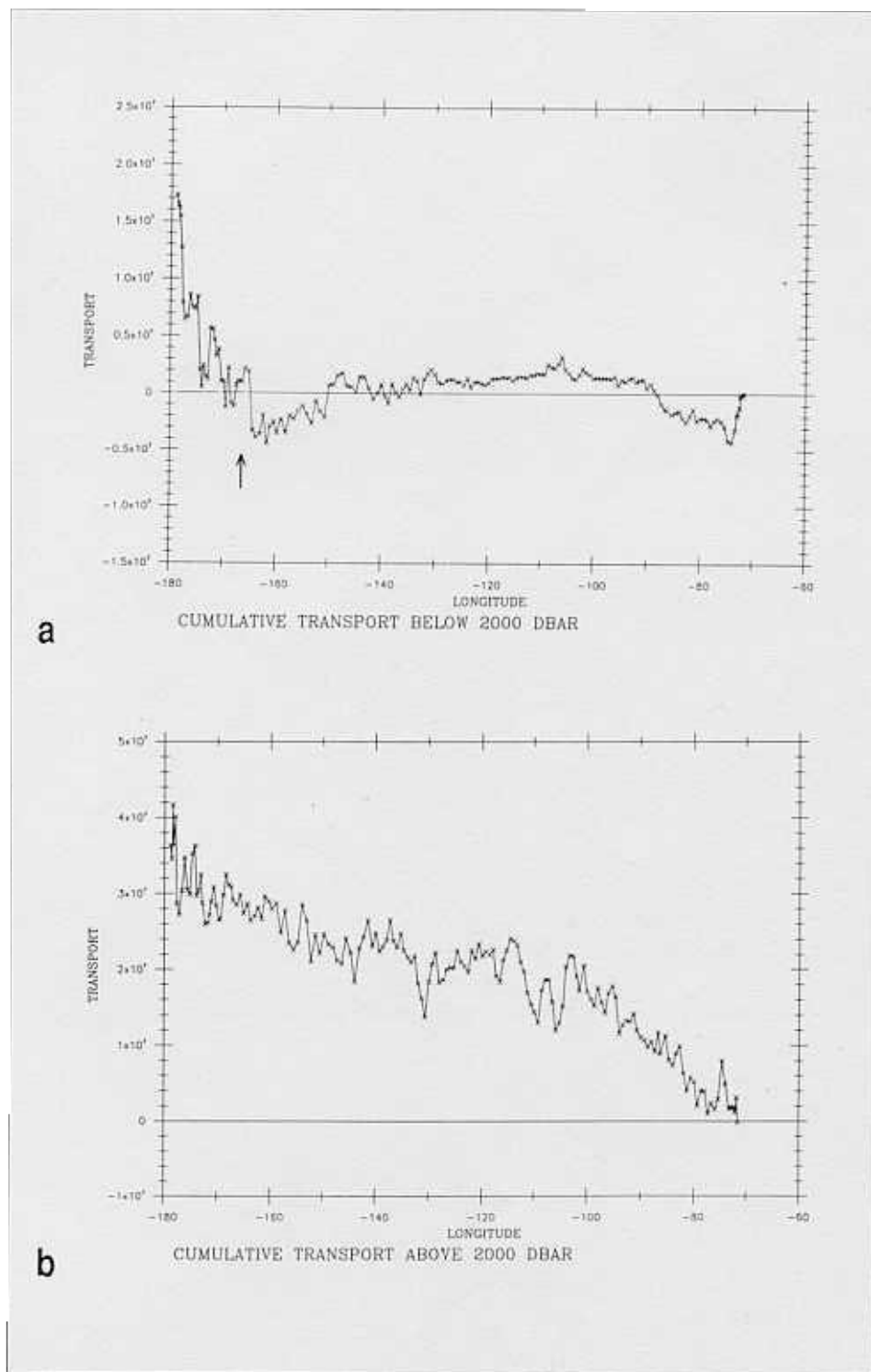


Figure 2. Transport for a first cut at a variable level of no motion by John Toole. Transport (a) below 2000 db, accumulated westward from Chile towards the Kermadec Ridge, (b) above 2000 db, accumulated westward from Chile towards the Kermadec Ridge. The arrow indicates the location of the eastern most mooring of the deep current meter array, PCM9, east of the Kermadec Ridge.

picks up, with a noisy but persistent accumulation of southward flow, the expected interior flow of abyssal circulation theory, with a magnitude of about  $6 \times 10^6 \text{ m}^3 \text{ s}^{-1}$ .

As the data came in during the cruise, we were struck by the width of the region of cold water associated with the DWBC east of the Kermadec Ridge. The accumulated  $6 \times 10^6 \text{ m}^3 \text{ s}^{-1}$  of southward interior flow is abruptly canceled by  $6 \times 10^6 \text{ m}^3 \text{ s}^{-1}$  of northward flow, substantially through one station pair near  $164^\circ\text{W}$ , where the first occurrence of water colder than potential temperature  $0.6^\circ\text{C}$  is found. This is well east of the western boundary of the basin: 1500 km east of the Kermadec Ridge. The Gebco bathymetric charts of this area are based on very sparse sounding data. The charts, however, do show an isolated deep spot near this station pair. This deep spot is oriented intriguingly to point south of east towards the area east of the Chatham Rise, where the cold water enters this basin from the south. We speculate, therefore, that some aspect of topographic channeling may be responsible for this apparent eastern branch of the DWBC. We have indicated by the arrow on Figure 2a the location of the eastern most mooring of the deep current meter array PCM9 to emphasize that a significant fraction (order 30%) of the DWBC's net transport passed east of the array at the time of this section.

The section crosses the Louisville Ridge chain of seamounts near  $172^\circ\text{W}$ , and Figure 2a shows a northward transport of  $7 \times 10^6 \text{ m}^3 \text{ s}^{-1}$  east of the Ridge partially compensated by a southward transport of  $5 \times 10^6 \text{ m}^3 \text{ s}^{-1}$  to its west. The narrow western intensified core of the DWBC still farther west transports northward about  $16 \times 10^6 \text{ m}^3 \text{ s}^{-1}$  in two distinct branches to either side of the Kermadec Trench, but without the major flow reversal in between found in the  $28^\circ\text{S}$  section by Warren (1973).

(continued on next page)

(P6, continued from previous page)

### The subtropical gyre and the subantarctic mode water

Figure 2b shows the transport above 2000 db accumulated eastward from the eastern boundary to the Kermadec Ridge, again for Toole's first cut at a level of no motion. This can be viewed as an estimate for the distribution of the transport of the subtropical gyre. The estimated net flow of  $35\text{--}42 \times 10^6 \text{ m}^3 \text{ s}^{-1}$  above 2000 db matches Godfrey's calculation of about  $40 \times 10^6 \text{ m}^3 \text{ s}^{-1}$  Sverdrup transport east of the date line at  $30^\circ \text{S}$  from the annual mean estimated wind stress distribution (Godfrey, 1989, his Figure 3). This is undoubtedly fortuitous, for there is nothing magical about the fraction of the net circulation that occurs above 2000 db, although that is the approximate maximum depth of the bowl structure of the thermocline usually associated with the wind driven gyre. Comparison of Figures 2a and 2b shows a combined net northward flow east of the Kermadec Ridge of order  $60 \times 10^6 \text{ m}^3 \text{ s}^{-1}$ , which may place too great a burden on the combined flow of the East Australian Current, the interior circulation between that Current and the Kermadec Ridge and the Indonesian throughflow to achieve overall mass balance. We will be in a good position to sort this all out due to the East Australian Current and DWBC moored array direct velocity measurements.

The lateral distribution of transport in the upper ocean, Figure 2b, includes various fairly intense and fairly resolved eddy disturbances and other elements of flow which will be examined in the future, so here we make only a few remarks.

At the eastern boundary a narrow northward flow of about  $11 \times 10^6 \text{ m}^3 \text{ s}^{-1}$  is immediately partially canceled by a southward flow of  $6 \times 10^6 \text{ m}^3 \text{ s}^{-1}$ , this gyre situated above the Chile Trench.

A curious W-shaped accumulated transport curve overlies the crest of the East Pacific Rise near  $110^\circ \text{W}$ , indicating a set of alternating partially resolved jets of magnitude  $5\text{--}10 \times 10^6 \text{ m}^3 \text{ s}^{-1}$ .

Near  $130^\circ \text{W}$  seven stations resolve a cyclonic (clockwise) eddy of width 450 km and transport amplitude  $8 \times 10^6 \text{ m}^3 \text{ s}^{-1}$ .

A substantial northward transport of narrow extent lies east of the Kermadec Ridge above the main axis of northward DWBC flow. Its intensity, however, is particularly sensitive to the reference level choice, as the shear here is strong throughout the water column.

On a scale broader than these jets and eddies, the basin scale circulation seems

banded, with substantially more northward transport accumulating in the eastern interior between the East Pacific Rise and Chile than in the western interior between the Kermadec Trench and the Rise. The image is perhaps one of an eastern concentration of the northward flow of the subtropical gyre. This concentration does not appear in estimated flow fields for the Sverdrup transport (cf. Godfrey, 1989), but it is a predictable impact of east-west basin elongation on the Sverdrup flow distribution when friction is included (Welander, 1976 and Bye and Veronis, 1978). On the other hand, an alternate description of the distribution of Figure 2a divides the region east

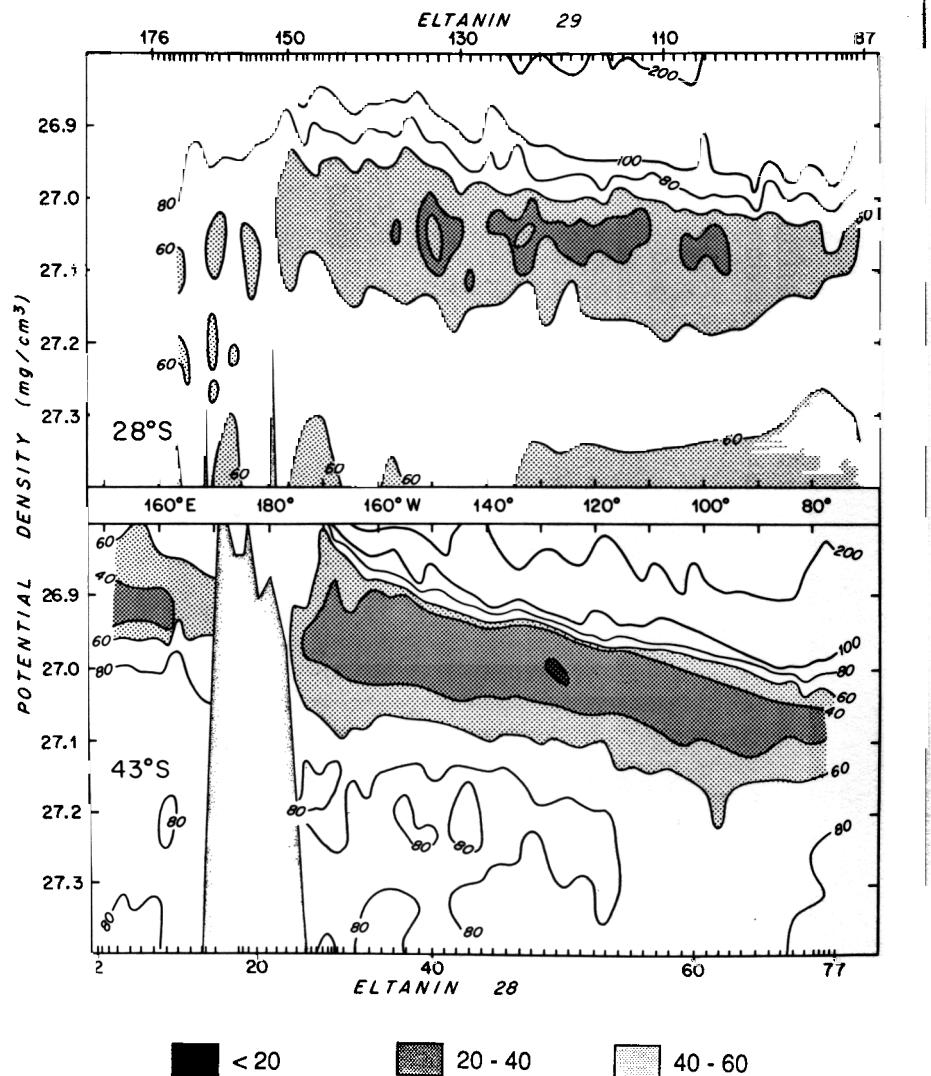


Figure 3. Potential vorticity ( $10^{-14} \text{ cm}^2 \text{ s}^{-1}$ ) for the Scorpio Expedition South Pacific transects at  $28^\circ \text{S}$  and  $43^\circ \text{S}$ , from McCartney, 1982.

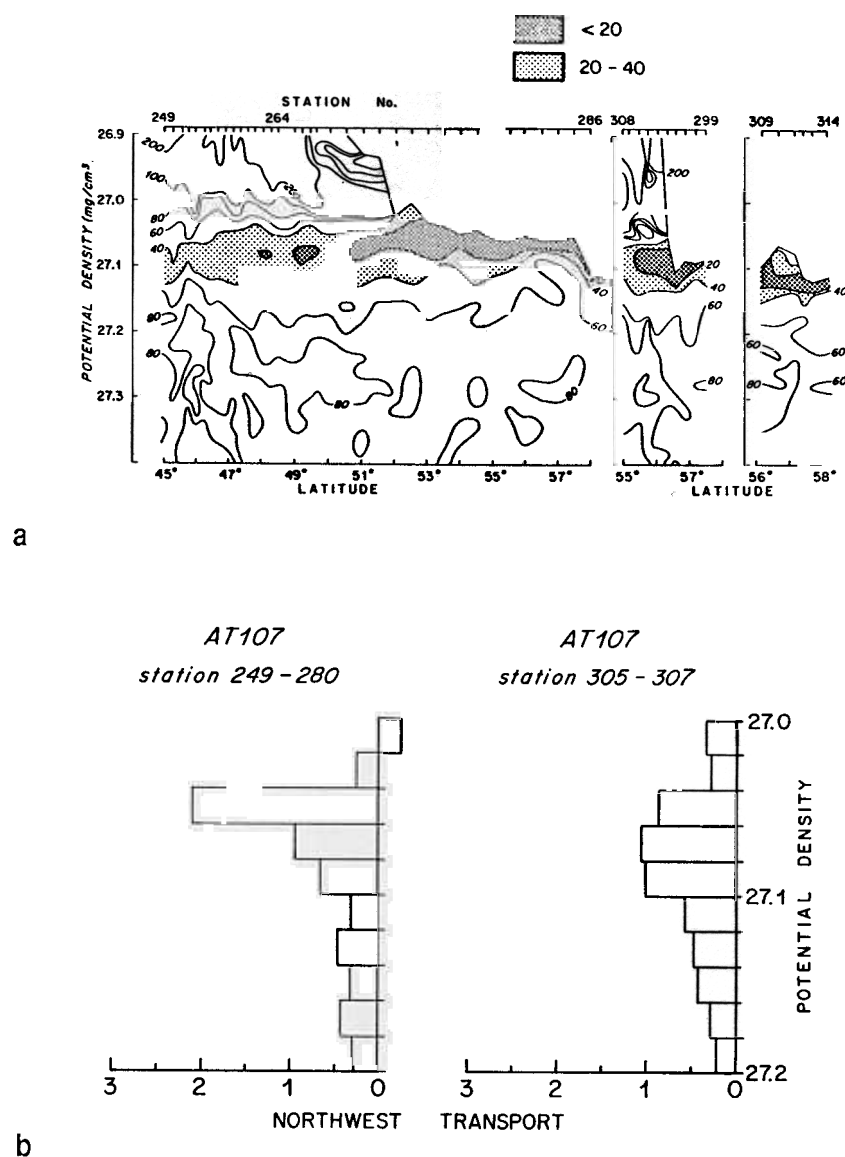


Figure 4. A late winter/early spring 1980 hydrographic survey of the southeastern South Pacific (Atlantis II) to define the densest varieties of Subantarctic Mode Water and their relation to the renewal of Antarctic Intermediate Water. (a) Potential Vorticity for comparison to Figure 3, and station locations. (b) Transport out of Subantarctic Zone into the subtropical gyre (level of no motion 2°C).

south of that latitude. Only the outermost streamlines of the gyre that acquire their SAMW in the southeastern South Pacific appear to sweep to this low a latitude.

Figure 4 establishes the connection of the denser modes that dominate from 28°S to the SAMW source region, with a set of sections from the Subantarctic Zone west of Drake passage taken in late winter/early spring 1980. Figure 4a shows the very low potential vorticity of the outcropping SAMW and its northwestward advection from that source region as a potential vorticity minimum core layer. The outcropping SAMW in these sections ranges from 5.1°C (27.05 EOS80) in the western section to 4.3°C (27.11 EOS80), all with salinity values near and below 34.20. Figure 4b quantifies the northwestward transport mode of the SAMW that flows from the southeastern source region for SAMW. About  $3.8 \times 10^6 \text{ m}^3 \text{ s}^{-1}$  of SAMW between 27.04 and 27.12 flows northwestward from this outcrop region into the subtropical gyre. Additional contributions from the subantarctic zone convection west of 90°W are expected to contribute SAMW transport to the subtropical gyre at densities lighter than 27.05.

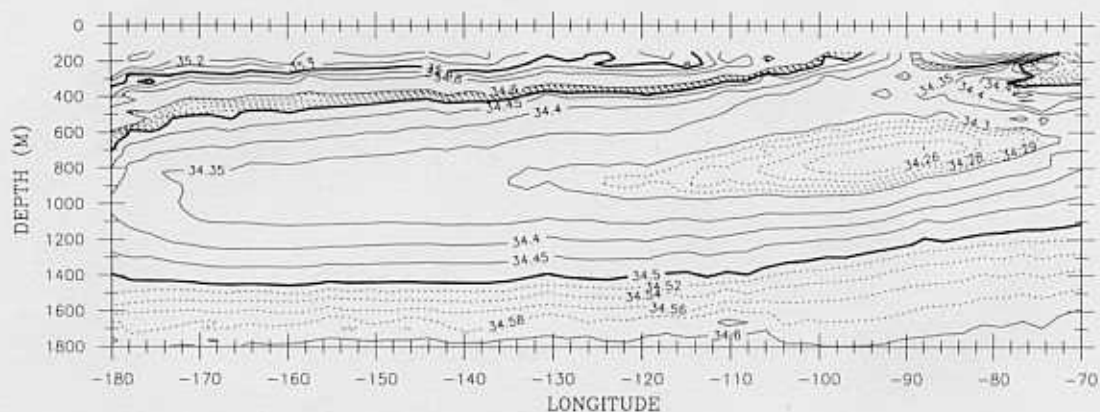
The new 32°S section, Figure 5a, shows a situation intermediate between the older Scorpio sections at 28°S and 43°S (Figure 3). Some of the lighter SAMW varieties that did not reach 28°S

(continued on next page)

of the Kermadec Ridge into thirds, with about half of the net transport in the eastern third, the other half in the western third, and almost no net flow in the central third. This central third overlies the broad crown of the East Pacific Rise.

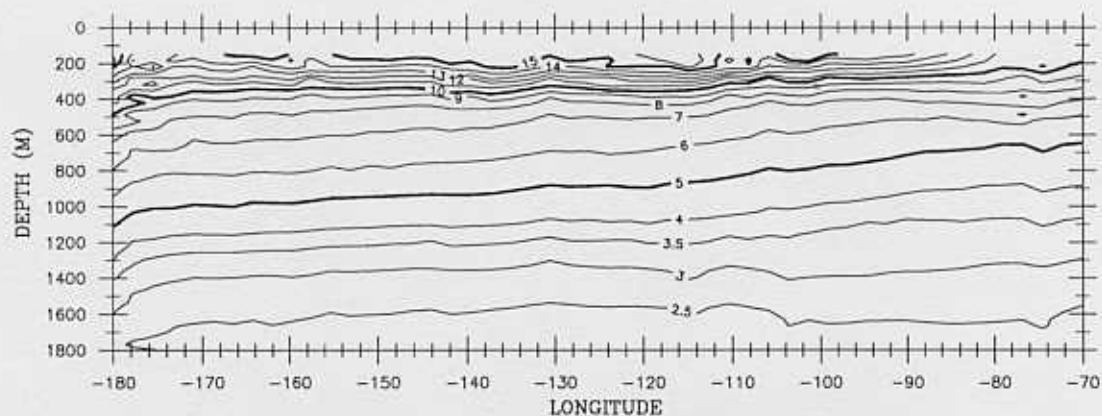
Circulating around the subtropical gyre of the South Pacific from their source region in the Subantarctic Zone are a range of Subantarctic Mode Waters (SAMWs) between 4°C and 9°C, or po-

tential density roughly 26.8–27.12 (McCartney, 1977 and 1982). Figure 3 illustrates the distribution of potential vorticity in the main thermocline for the Scorpio expedition sections. At 43°S the full range of SAMW varieties is swept through the section by the subtropical gyre circulation. The lighter varieties of SAMW sweeping through the 43°S section do not reach 28°S, indicating a subtropical closure of their gyre circulation



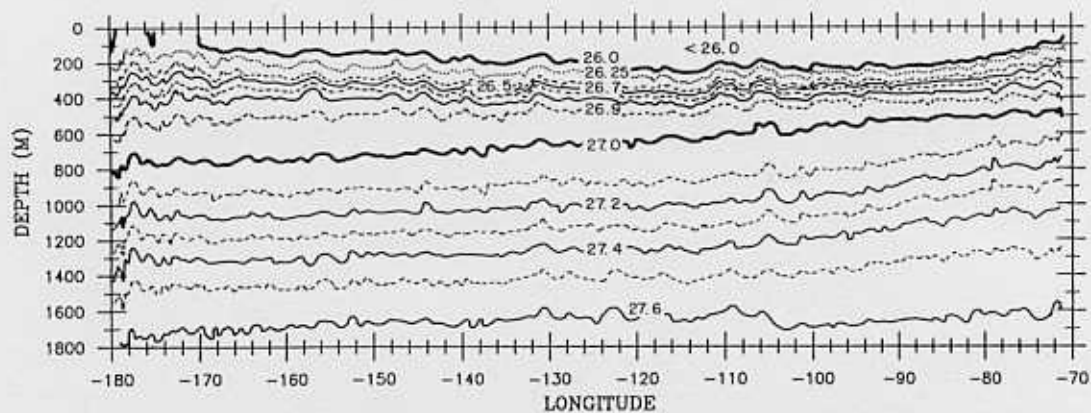
SALINITY (PSU), PACIFIC 32S

a



POTENTIAL TEMPERATURE (DEG C), PACIFIC 32S

b



POTENTIAL DENSITY PACIFIC 32°S

c



(P6, continued)

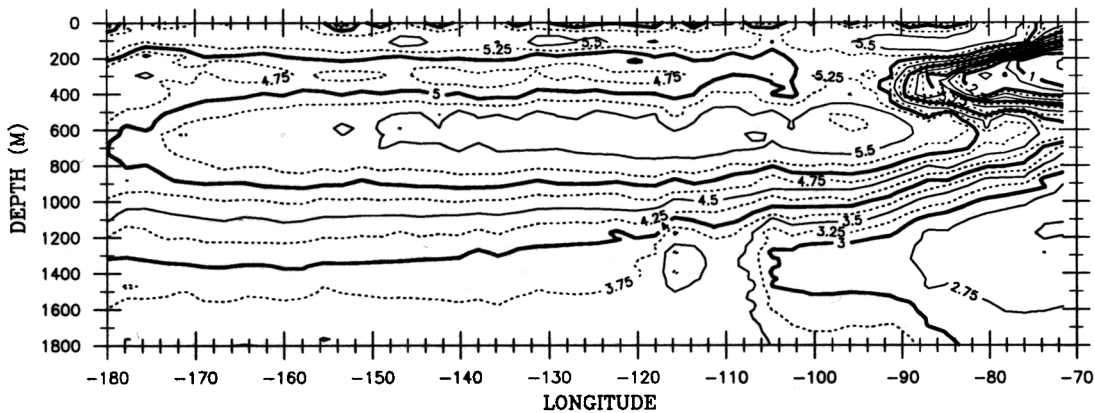
do pass through 32°S, but the denser varieties in the east are predominantly clear. The SAMW core surface is near 5°C in the east, with a progressive westward shift to varieties near 7°C at the Kermadec Trench. These lighter modes form in the Subantarctic zone near New Zealand, and have a circulation restricted to the area west of the East Pacific Rise. The convective origin of the SAMW is reflected in the coincidence of the low potential vorticity and oxygen maximum

core layers. The base of the SAMW layer can be taken as the potential vorticity maximum layer (exceeding  $70 \times 10^{-14} \text{ cm}^{-1} \text{ s}^{-1}$ ) that centers on 4.0°C or 27.2 potential density. Above that level the relative influence of subantarctic zone convection increases upwards to a maximum influence at the core layer center.

One of the primary goals of our work is to describe the South Pacific distribution of SAMW from these and other WHP data, and from the historical data,

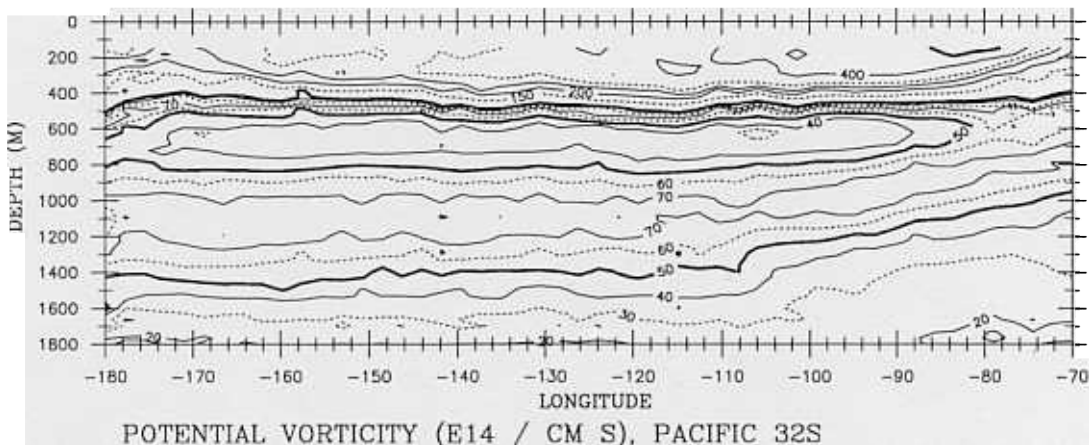
and relate the distribution to the circulation and ventilation of the subtropical gyre. Of particular interest is describing the pathways by which the various SAMW varieties fold under each other as they circle the subtropical gyre, in other words, relating the SAMW distribution to the spiraling of the geostrophic flow with increasing depth (density). One possible framework for thinking about this circulation

(continued on bottom of next page,



OXYGEN (ML / L), PACIFIC 32S

d



POTENTIAL VORTICITY (E14 / CM S), PACIFIC 32S

e

Figure 5, left and above. Upper ocean property distributions for the 32°S section between the Kermadec Ridge and Chile (machine contoured, beware artifacts at the eastern and western extremes).

(P6, continued from previous page)

tion is the ventilated thermocline theory as applied to the South Pacific, with due consideration to processes at the eastern boundary (de Szoeke, 1987 and 1992).

This description will include the relationship between the SAMW and the Antarctic Intermediate Water (AAIW)—the salinity minimum core surface and the waters immediately above and below that surface. At 32°S the AAIW core surface (salinity minimum) lies beneath the core surface of the SAMW (potential vorticity minimum), Figure 5. But the AAIW and SAMW layers overlap throughout the section. For example, the high potential vorticity ridge ( $> 70 \times 10^{-14} \text{cm}^{-1}\text{s}^{-1}$ ) that defines the base of the SAMW ventilated layer lies well beneath the AAIW core. The core surfaces become vertically close but not coincident east of about 110°W

along the 32°S section, with the eastern intensification of the AAIW strength evident. Following on the hypothesis by McCartney (1977 and 1982), as supported by the survey shown in Figure 4, that the densest SAMW (about 27.11) forms the core surface of the South Pacific AAIW, we are now examining how this winter outcropping layer freshens the part of the AAIW layer beneath the core surface. The freshening occurs because of vertical diffusion from the outcropping SAMW in the southeastern Pacific, which is lower in salinity, higher in oxygen, and lower in potential vorticity than the denser levels of the AAIW of that region. In other words, the outcropping SAMW varieties, Figure 4, with low potential vorticity, low salinity and high oxygen, ventilate the unexposed part of the salinity minimum

layer denser than 27.11 by vertical diffusion, as the unexposed part is higher in salinity and lower in oxygen and thus susceptible to freshening by down-gradient diffusion. Some numerical models show patterns similar to this observed AAIW/SAMW formation and circulation, with their focal point for AAIW source flow being just west of Drake Passage as suggested by Figure 4 (Bryan and Lewis, 1979, and Bryan, personal communication, 1982, and more recently by a series of studies by England, 1992 and England *et al.*, 1992 and 1993).

## References

- Bryan, K. and Lewis, L.J., 1979. A water mass model of the World Ocean. *J. Geophys. Res.*, 85(C5), 2503–2517.
- Bye, J.A.T., and G. Veronis, 1978. A correction of the Sverdrup Transport. *J. Phys. Oceanogr.*, 9, 647–654.
- de Szoeke, R.A., 1987. On the wind-driven circulation of the South Pacific Ocean. *J. Phys. Oceanogr.*, 17, 613–630.
- de Szoeke, R.A., 1992. Effects of along-shore wind stress at the eastern boundary on circulation in the ocean pycnocline. *J. Phys. Oceanogr.*, 22, 247–268.
- England, M.H., 1992. On the formation of Antarctic intermediate and bottom water in ocean general circulation models. *J. Phys. Oceanogr.*, 22, 918–926.
- England, M.H., M. Tomczak, and J.S. Godfrey, 1992. Water-mass formation and Sverdrup dynamics; a comparison between climatology and a coupled ocean-atmosphere model. *J. Mar. Systems*, 3, 279–306.
- England, M.H., J.S. Godfrey, A.C. Hirst, M. Tomczak, 1993. The mechanism for Antarctic intermediate water renewal in a world ocean model. *J. Phys. Oceanogr.*, in press.
- Godfrey, J. S., 1989. A Sverdrup model of the depth integrated flow for the world ocean allowing for island circulations. *Geophys. Astrophys. Fluid Dyn.*, 45, 89–112.
- McCartney, M.S., 1977. Subantarctic mode water. In: *A Voyage of Discovery*. M. Angel, Ed., Pergamon Press, 103–119.
- McCartney, M.S., 1982. The subtropical recirculation of Mode Waters. *J. Mar. Res.*, Supplement to 40, 427–464.
- Reid, J.L., 1973. Transpacific hydrographic sections at latitudes 43°S and 28°S in the Scorpio Expedition - III. Upper water and a note on southward flow at mid-depth. *Deep Sea Res.*, 20, 39–49.
- Warren, B.A., 1973. Transpacific hydrographic sections at Lats. 43°S and 28°S: The SCORPIO Expedition - II. Deep water. *Deep Sea Res.*, 20, 9–38.
- Welander, P., 1976. A zonally uniform regime in the oceanic circulation. *J. Phys. Oceanogr.*, 6(2), 121–124. ■